Supporting Information

Tuning Defects in Cu_2O Nanostructure via Room Temperature Mechanical Pressing: Impacts on Defect-Dependant Optical and Photoelectrochemical Sensing Performances

Yun Cai,[a] Wenyao Zhou,[a] Hongli Wang,[a] Jiajie Bi,[ab] Fengjiao Yu,[a] Jun Fang[a] and Yang Yang*[a]*

[a] State Key Laboratory of Materials-Oriented Chemical Engineering, College of Chemical Engineering, Nanjing Tech University, Nanjing 211816, China

* Email: yangy@njtech.edu.cn

[b] College of Chemistry and Materials Engineering, Wenzhou University, Wenzhou, Zhejiang, 325035, China

* Email: bjj@wzu.edu.cn

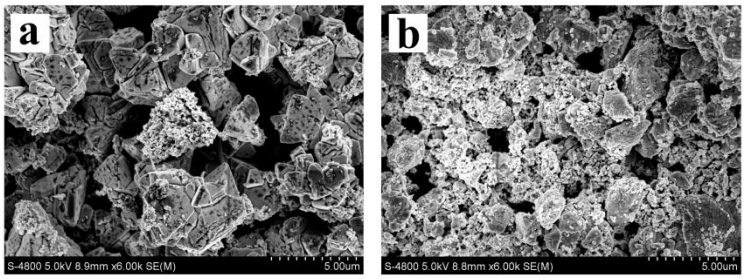

Fig. S1 SEM images of (a) D-powder and (b) P-powder subjected to the mechanical pressing at a pressure of 0.36 GPa.

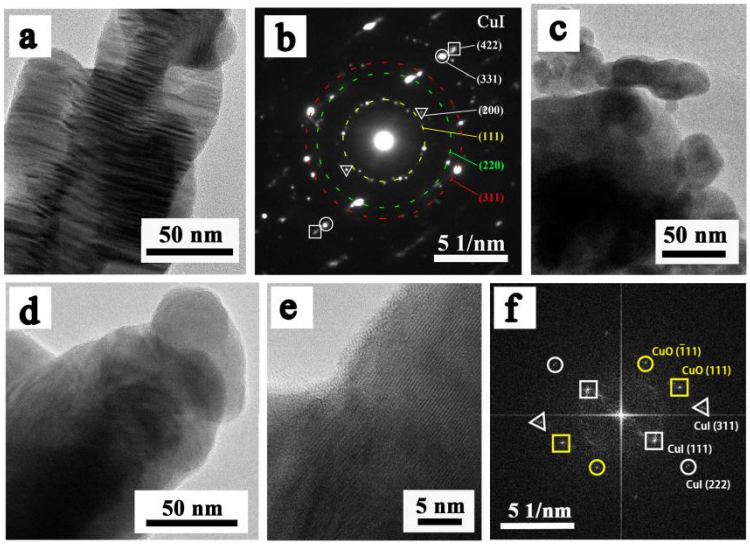

Fig. S2 (a) TEM image and (b) corresponding SAED pattern of D-powder. (c) TEM image of P-powder. (d) TEM image, (e) HRTEM image and (f) FFT pattern calculated from (e) of A-powder.

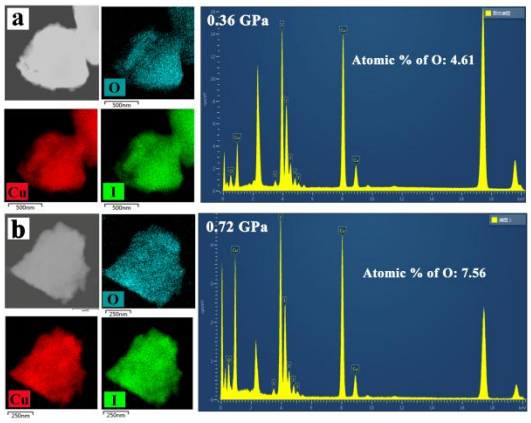

Fig. S3 STEM images, EDS elemental mapping images and atomic percentages of O of the samples pressured under 0.36 GPa (a) and 0.72 GPa (b).

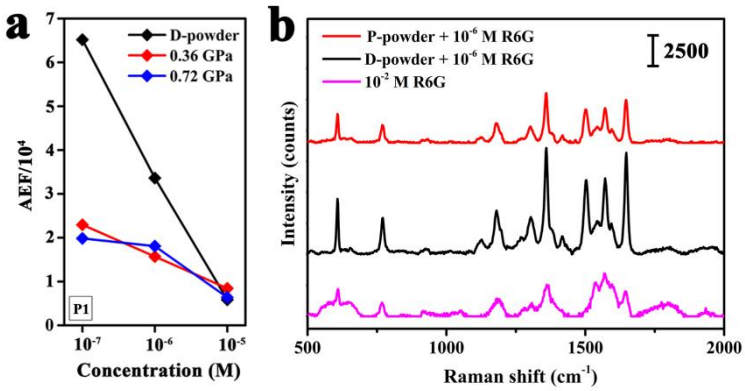

Fig. S4 (a) Statistical evolution of the analytical enhancement factors (AEFs) as a function of R6G concentration. (b) Raman spectra of R6G at a concentration of 1.0×10^{-2} M collected on a Si wafer and R6G at a concentration of 1.0×10^{-6} M collected on the Si wafer deposited with D-powder and P-powder, respectively.

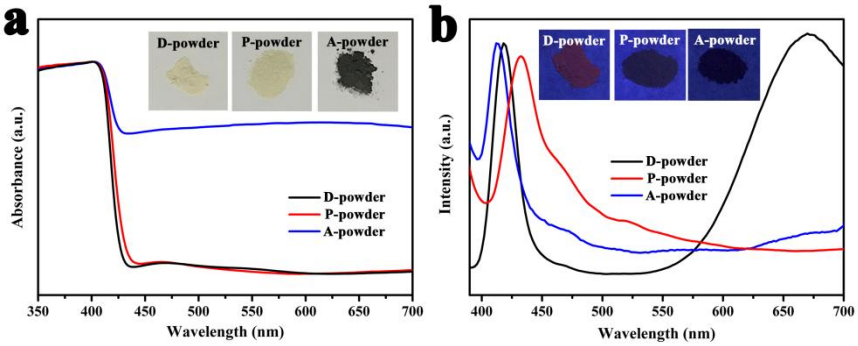

Fig. S5 (a) UV–vis diffuse reflectance spectra of D-powder, P-powder and A-powder; inset in (a) is the corresponding photographs under natural light. (b) PL spectra of the aforementioned samples acquired with a 365 nm excitation wavelength; inset in (b) is the corresponding fluorescence images under UV lamp (365 nm) irradiation.

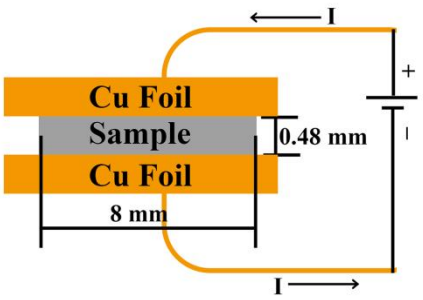

Fig. S6 Schematic illustration of conductivity measurements.

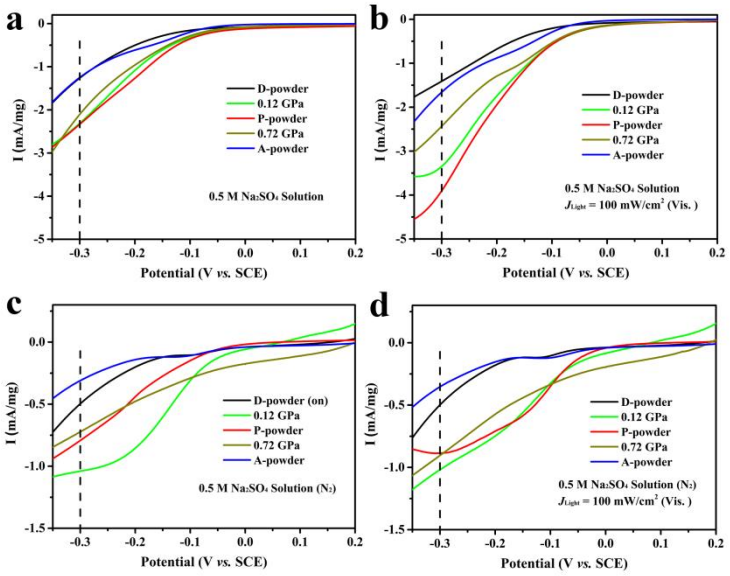

Fig. S7 Linear sweep voltammograms (LSVs) of the different samples in 0.5 M Na_2SO_4 solution with dissolved oxygen in dark (a) and under visible light illumination (b), and without dissolved oxygen in dark (c) and under visible light illumination (d).

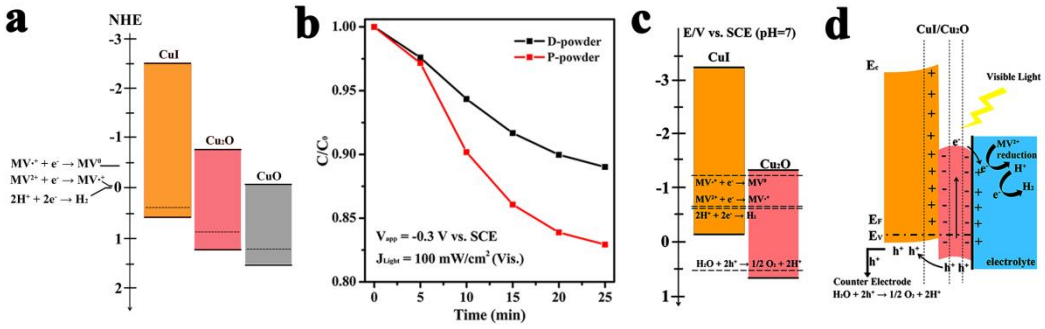

Fig. S8 (a) Energy levels of CuI, Cu_2O and CuO. (b) PEC degradation of $MVCl_2$ (10 μM) by D-powder and P-powder in an oxygen-free environment under visible light. (c) Band alignment of Cu_2O and CuI before equilibration. (d) Schematic illustration of PEC reduction reactions catalyzed by P-powder in an oxygen-free environment under visible light illumination.